The speed law for highly radiative flames in a gaseous mixture with large activation energy*

Jan Bouwe van den Berg
Department of Mathematics, Vrije Universiteit, De Boelelaan 1081
1081 HV Amsterdam, The Netherlands
E-mail: janbouwe@few.vu.nl

Claude-Michel Brauner
Mathématiques Appliquées de Bordeaux, Université Bordeaux I
33405 Talence cedex, France
E-mail: brauner@math.u-bordeaux.fr

Josephus Hulshof
Department of Mathematics, Vrije Universiteit, De Boelelaan 1081
1081 HV Amsterdam, The Netherlands
E-mail: jhulshof@few.vu.nl

Alessandra Lunardi
Dipartimento di Matematica, Università di Parma
Via D'Azeglio 85/A, 43100 Parma, Italy
E-mail: lunardi@prmat.math.unipr.it

*This work was supported by a CNRS/NWO grant and the RTN network Fronts-Singularities, HPRN-CT-2002-00274. JH is also supported by the CWI in Amsterdam, and JB is also supported by NWO. We thank Guy Joulin for very fruitful discussions.

Abstract

We study a thermo-diffusive combustion model for premixed flames propagating in reactive gaseous mixtures which contain inert dust. As observed by Joulin, radiative transfer of heat may significantly enhance the flame temperature and its propagation speed. The Joulin effect is at its most pronounced in the parameter regime where the medium is very transparent while radiative flux dominates convection. In this asymptotic regime, where in the limit the flame temperature achieves its upper bound, we determine the law that describes the relation between the propagation speed of the flame and the control parameters. Finally we present strong numerical evidence for the validity of the asymptotic analysis.

1 Introduction

Combustion is one of the important phenomena in our world. It occurs in controlled applications such as rocket engines, energy plants and cooking on natural gas, as well as in forest fires and mine and tunnel accidents. Experiments in combustion research are both difficult and expensive, which underlines the need for good mathematical models and their analysis.

Combustion models are based on the incorporation of different physical and chemical principles, expressed in the language of mathematics. Simplifying, sometimes heuristic, assumptions are unavoidable to make mathematical treatment possible, be it by numerical, formal asymptotic or analytical methods. In the latter the modern theory of infinite-dimensional dynamical systems and its application to free boundary problems plays an important role. Such free boundary problems (FBPs) occur as various flame front models. Asymptotic arguments are strongly intertwined with the derivation of such FBPs from physical and chemical principles.

In this paper we study a thermo-diffusive combustion model for premixed flames propagating in reactive gaseous mixtures which contain inert dust that radiates thermal energy. Radiative transfer of heat involves both emission and absorption of radiation, and may significantly influence the flame temperature, its propagation speed, and the flammibility of the medium itself. This is the so-called Joulin effect [13, 5]: the propagation speed increases compared to a similar flame without radiation and there is a temperature overshoot at the flame front. A radiative flame can be ignited at a lower external temperature than a non-radiative flame.

The Joulin effect is at its most pronounced in the parameter regime where the medium is very transparent while radiative flux dominates convection. In this asymptotic regime our goal is to determine the law that describes the relation between the propagation speed of the flame and the control parameters.

In Section 2 we will discuss the model in more detail. For now, we just highlight the most important features. Following Buckmaster, we formulate the thermal-diffusive model with the thin reactive flame zone replaced by a free boundary. At the free boundary the normal derivative of the (normalised) temperature T is related to the reaction rate ω, which is given by an Arrhenius type law:

$$\omega = A \exp\left(-\frac{N}{T^*}\right). \tag{1}$$

Here N is the activation energy, T^* is the temperature at the free boundary, and A is a so-called pre-exponential constant, which will be specified later.

As a model for the radiative field, we take the Eddington equation, which contains two important radiative parameters: the (dimensionless) opacity α and the Boltzmann number β, a measure of the radiative energy flux compared to the convective flux.

Flames will be modelled as travelling waves propagating into the fresh region where the fuel mass fraction and the temperature are constant, Y_- for the fuel mass fraction, T_- for the temperature. A conservation law implies that the temperature T_+ far behind the flame front is given by

$$T_+ = T_- + Y_-.$$

Depending on the opacity of the medium, radiation may significantly influence the flame profile, see [12, 3, 5]. *Radiative flames* are characterised by an overshoot of the flame temperature T^* as well as an enhancement in the burning rate and flame speed μ, which is given by

$$\mu = \frac{\omega}{Y_-}. \tag{2}$$

In [4] it was proved that the flame temperature T^* is bounded by

$$T_- + Y_- < T^* < T_- + 2Y_-.$$

These bounds, which were already conjectured in [5], are achieved in certain limits. The lower bound is in fact the flame temperature in absence of radiation (the "adiabatic" case), and it is approached as $\alpha \to \infty$ or $\beta \to 0$ (see [4]). In the present paper, however, we focus on the combined asymptotic regime

$$\alpha \to 0, \tag{3a}$$

$$\beta \to \infty, \tag{3b}$$

$$\alpha\beta \to 0, \tag{3c}$$

because in this regime the flame temperature approaches the upper bound, i.e.

$$\text{in the limit (3):} \qquad T^* \to T_- + 2Y_-, \tag{4}$$

and the radiative effects are most pronounced.

We are going to combine this asymptotic regime of the radiative parameters with the high activation limit, i.e., we take

$$\varepsilon = \frac{1}{N}$$

as the main small parameter. This is very much in the same spirit as the Near-Equidiffusional Flame (NEF) approximation that is frequently used in the absence of radiative effects, see

[15]. There the reciprocal ε of the activation energy is coupled to the Lewis number. Here we couple ε to the radiative parameters.

Of primary physical interest are flames that, in this asymptotic regime, propagate with a finite velocity μ. In view of (2) μ is proportional to the reaction rate ω given in (1). Hence, in the high activation limit $N = \varepsilon^{-1} \to \infty$, finite speeds of propagation can be obtained provided A is of the order $\exp(N/T_c)$, where T_c is a characteristic temperature, to be fixed shortly. Indeed, since in this notation

$$\mu = \frac{1}{Y_-} \exp\left(\frac{1}{\varepsilon}\left(\frac{1}{T_c} - \frac{1}{T^*}\right)\right), \tag{5}$$

the characteristic temperature T_c should equal the asymptotic value of the flame temperature T^*, hence in view of (4) the only possibility is

$$T_c = T_- + 2Y_-.$$

This is the upper extreme of T_* and it stands in sharp contrast with the NEF approach, where the suitable choice for T_c is the lower extreme, namely $T_- + Y_-$.

Since we want to look at the asymptotic regime where simultaneously the reciprocal ε of the activation energy tends to zero and the radiative parameters α and β behave as given in (3), we have to couple α and β to ε. Limit condition (3c) suggests it is convenient to introduce the combined parameter

$$\chi \stackrel{\text{def}}{=} \alpha\beta.$$

Our results show that an asymptotically *finite* propagation speed requires

$$\chi = O(\varepsilon) \qquad \text{and} \qquad \beta^{-1} = O(\varepsilon^{1/2}). \tag{6}$$

Since α has a more direct physical meaning than χ, let us give an alternative formulation of these conditions. For simplicity we assume that both α and β are (asymptotically) powers of ε:

$$\alpha \sim \alpha_0 \varepsilon^a \qquad \text{and} \qquad \beta \sim \beta_0 \varepsilon^{-b}.$$

The connection with (6) is made through

$$\chi = \alpha\beta = \alpha_0\beta_0\varepsilon^{a-b} \sim \chi_0 \varepsilon^{a-b}.$$

To obtain a finite flame velocity one the of following four possibilities must hold (see also Figure 1):

$$\begin{array}{rlll}
\text{I:} & a = \frac{3}{2} & \text{and} & b = \frac{1}{2}; \\
\text{II:} & a > \frac{3}{2} & \text{and} & b = \frac{1}{2}; \\
\text{III:} & a = b + 1 & \text{and} & b > \frac{1}{2}; \\
\text{IV:} & a > b + 1 & \text{and} & b > \frac{1}{2}.
\end{array}$$

We remark that the special scaling $\alpha \sim \alpha_0 \varepsilon^{3/2}$ and $\beta \sim \beta_0 \varepsilon^{1/2}$ in case I was first observed by Joulin and Eudier [13].

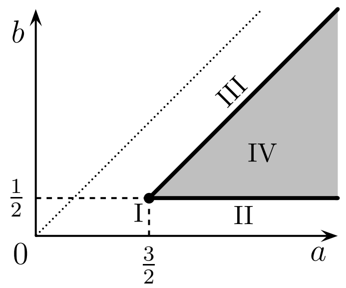

Figure 1: The asymptotic regime under consideration in terms of the exponents a and b. The area below the dotted line corresponds to radiation dominated flames (3). Finite wave speeds are found in the shaded region and, more significantly, on its boundary.

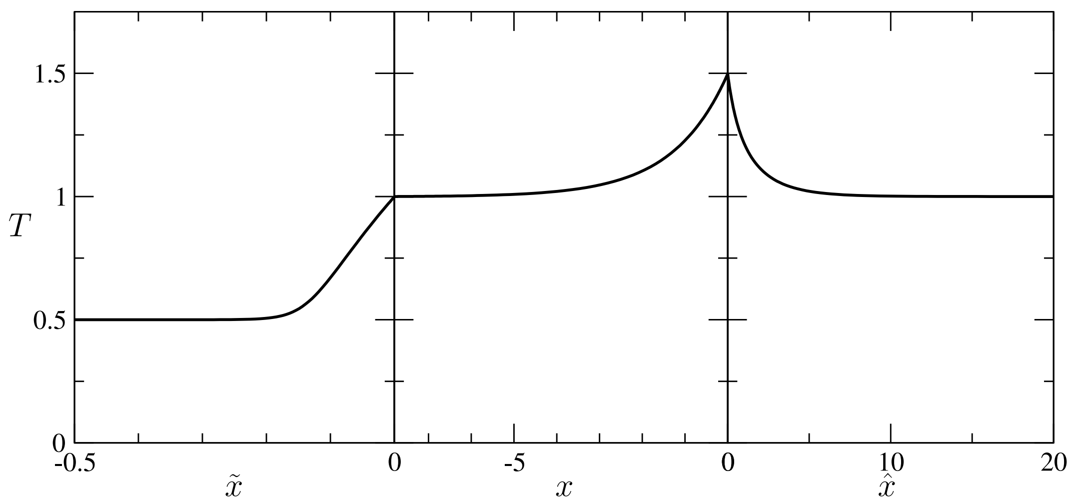

Figure 2: In the combined asymptotic limit of high activation energy $\varepsilon \to 0$ coupled to the radiative parameters $\alpha = \alpha_0 \varepsilon^a$ and $\beta = \beta_0 \varepsilon^{-b}$ with $b \geq \frac{1}{2}$ and $a \geq b + 1$ the solution profile separates into three spatial scales. The numerical solution shown is for $\varepsilon = 0.001$, $\alpha = 0.3\varepsilon^{3/2}$, $\beta = 0.3\varepsilon^{-1/2}$ and $T_- = Y_- = 0.5$. Notice that the scales are very different in the three regions since on the left the variable is $\tilde{x} = \alpha\beta^{-1}x$, in the middle it is x, while on the right it is $\hat{x} = \alpha\beta x$.

In the limit (3) the flame profile naturally separates into three spatial scales (see also Figure 2):

$$x, \qquad \hat{x} = \alpha\beta\, x, \qquad \tilde{x} = \frac{\alpha}{\beta}\, x, \tag{7}$$

where x is the spatial variable in a co-moving frame (with speed μ). In Section 3 we will perform a matching analysis of these three scales. This enables us to derive a law for the asymptotic speed μ of the front. In the four cases identified above the speed law reads (with $T_+ = T_- + Y_-$)

$$\text{I:} \qquad \ln(\mu\, Y_-) = -\frac{\alpha_0\beta_0 T_+^2}{\mu^2} E_1\Big(\tfrac{Y_-}{T_+}\Big) - \frac{\mu^2}{\beta_0^2 T_+^7} E_2\Big(\tfrac{Y_-}{T_+}\Big); \tag{8a}$$

$$\text{II:} \qquad \ln(\mu\, Y_-) = - \frac{\mu^2}{\beta_0^2 T_+^7} E_2\Big(\tfrac{Y_-}{T_+}\Big); \tag{8b}$$

$$\text{III:} \qquad \ln(\mu\, Y_-) = -\frac{\alpha_0\beta_0 T_+^2}{\mu^2} E_1\Big(\tfrac{Y_-}{T_+}\Big); \tag{8c}$$

$$\text{IV:} \qquad \ln(\mu\, Y_-) = 0. \tag{8d}$$

Here

$$E_1(s) = \frac{8s + 9s^2 + \frac{16}{3}s^3 + \frac{5}{4}s^4}{(1+s)^2},$$
$$E_2(s) = \frac{3s}{16(1+s)^2} + \frac{3}{4(1+s)^2}\int_0^s \frac{t\,dt}{(1+t)^4 - 1}.$$

It is clear that case I is central to the whole analysis and the other cases are fairly straightforward reductions. On the other hand, in the asymptotic analysis presented in Section 3 we will in some sense compute cases II and III and then combine them to obtain case I. The last case IV is rather boring, since there is just one finite velocity, namely $\mu = 1/Y_-$.

We remark that in the whole asymptotic regime (3) the profile of any travelling wave with finite speed of propagation (in the asymptotic limit $\varepsilon \to 0$) decomposes into the three different spatial scales (7). The asymptotic analysis in Section 3 is thus valid for the whole parameter regime of radiation dominated flames. In Figure 1 this corresponds to the area below the dotted line. The fact that in only part of this parameter regime finite wave speeds occur is merely a consequence of the way the wave speed is related to T^* and ε (i.e. via (5)).

The organisation of the paper is as follows. In Section 2 we introduce the mathematical model and we make the reduction to a travelling wave problem. In Section 3.1 we explain how the matched asymptotic analysis works, while in Sections 3.2–3.4 the calculations are performed, i.e., we analyse the profile in three different spatial scales and match these to obtain the full asymptotic picture. This also leads us to the formula for the speed law presented above. Finally, in Section 4 we look in more detail at the speed law, we compare with numerical computations, and we draw conclusions about the bifurcation diagrams.

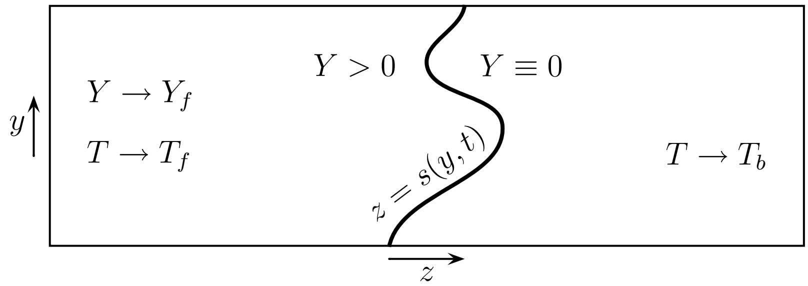

Figure 3: The geometric setting of the propagating flame.

2 Models and equations

2.1 Premixed flame propagation with constant opacity

We introduce the thermo-diffusive combustion model with constant density, simple chemistry and large activation energy, for a premixed flame propagating in a reactive gaseous mixture. We incorporate the flux of the thermal radiative field generated by the radiation of dust particles. The geometric setting is the following (see also Figure 3): the flame propagates into the *fresh* region, where, far ahead of the flame front ($z \to -\infty$), the fuel mass fraction Y and the temperature T are constant:

$$\lim_{z\to-\infty} Y(z) = Y_f \qquad \text{and} \qquad \lim_{z\to-\infty} T(z) = T_f$$

The region of the flame where the reaction occurs is infinitesimally thin and is located at $z = s(y,t)$, the free boundary of the problem, y being the lateral two-dimensional variable. To the right of the free boundary all fuel has been burnt ($Y(z) = 0$ for $z \geq s(y,t)$) and far behind the flame front the temperature approaches the *burnt* temperature $T_b = \lim_{z\to\infty} T(z)$. The time-dependent system of equations for mass fraction Y and temperature T reads

$$\frac{\partial}{\partial t}(\rho Y) - \nabla(\rho D \nabla Y) = 0, \quad z < s(y,t); \qquad Y = 0, \quad z \geq s(y,t); \tag{9a}$$

$$\frac{\partial}{\partial t}(\rho C_p T) - \lambda \Delta T + \nabla \cdot \mathbf{F_R} = 0, \quad z \neq s(y,t). \tag{9b}$$

The physical parameters are the diffusion constant D, the heat conduction coefficient λ and the specific heat C_p and the density ρ of the gas (part of which is fuel). The divergence of the radiative energy flux $\mathbf{F_R}$ appears as a loss term in the temperature equation (9b). At the flame front, the jump conditions for the normal derivatives

$$\rho D \left[\frac{\partial Y}{\partial n}\right] = \omega(T); \quad \lambda \left[\frac{\partial T}{\partial n}\right] = -Q\omega(T), \qquad \text{at } z = s(y,t), \tag{9c}$$

are imposed to balance the heat flux coming out of the flame with the mass flux going into the flame, the reaction heat Q being the proportionality constant between the two. These fluxes are also coupled to the chemical reaction rate ω, for which we take a simple Arrhenius law. In the free boundary approximation it reads

$$\omega = A \exp\left(-\frac{E}{2RT^*}\right). \tag{9d}$$

Here T^* denotes the temperature at the flame front, and the other constants are the gas constant R, the activation energy E, and the "pre-exponential" factor A. Note that the factor 2 in the reaction rate is a consequence of the derivation of the free boundary jump conditions from the reaction-diffusion formulation, see [8].

As a law for the radiative flux $\mathbf{F_R}$ we take the Eddington equation

$$-L^2\nabla(\nabla\cdot\mathbf{F_R}) + 3\mathbf{F_R} + 4\sigma_{\mathrm{sb}}L\nabla T^4 = 0, \tag{9e}$$

where σ_{sb} is the Stefan-Boltzmann constant and L is the mean free path length of the photons. In astrophysics the Eddington equation is a well-known approximation to the radiative field [11, 17, 16]. It is a good approximation when scattering is nearly isotropic, particularly in a one-dimensional setting. The travelling waves that we use as a model for the propagating flames have indeed a one-dimensional structure. Since the radiative transfer plays a central role in our model, we give some some insight in the derivation of the Eddington equation in the Appendix.

We emphasise that the Eddingtion equation models radiative transfer rather than radiative heat losses. There is however an asymptotic limit, discussed in [4, 1], where the radiative flux is given by $\nabla\cdot\mathbf{F_R} = \frac{4\sigma_{\mathrm{sb}}}{L}(T^4 - T_b^4)$. This asymptotic limit thus looks like heat loss to a reservoir held at $T = T_b$. It can be compared to the usual radiative heat loss models (see [18, Sec. 8.2], [6, p. 43]) that are based on the law $\nabla\cdot\mathbf{F_R} = \frac{4\sigma_{\mathrm{sb}}}{L}(T^4 - T_f^4)$, which differs only in the temperature of the reservoir (T_f instead of T_b).

2.2 Dimensionless variables

We now make the system of equations (9) dimensionless and scale out many of the parameters. We define non-dimensional temperature $\hat{T}$, radiative flux $\hat{\mathbf{F}}_\mathbf{R}$, time $\hat{t}$ and spatial coordinate $\hat{\mathbf{r}}$ by comparison with suitable chosen reference quantities indexed by s:

$$\hat{t} = \frac{t}{t_s}, \quad \hat{\mathbf{r}} = \frac{\mathbf{r}}{r_s}, \quad \hat{T} = \frac{T}{T_s}, \quad \hat{\mathbf{F}}_\mathbf{R} = \frac{\mathbf{F_R}}{F_s}.$$

We choose the reference quantities such that they satisfy the following set of equations:

$$\frac{\lambda t_s}{\rho C_p r_s^2} = 1, \quad \frac{4\sigma_{\mathrm{sb}}T_s^4}{F_s} = 1, \quad \frac{\rho D}{B r_s} = 1, \quad \frac{\lambda T_s}{QBr_s} = 1,$$

that is

$$F_s = \frac{4\sigma_{\mathrm{sb}}Q^4D^4\rho^4}{\lambda^4}, \quad T_s = \frac{QD\rho}{\lambda}, \quad t_s = \frac{\rho^3 C_p D^2}{\lambda B^2}, \quad r_s = \frac{D\rho}{B}.$$

Here B is defined by

$$A = B\exp\left(\frac{E}{2RT_C}\right),$$

where T_C is the characteristic temperature. The necessity of this splitting of the pre-exponential factor A has already been discussed in the introduction. In the high activation energy asymptotics that we are going to employ it is widely used, see for example [6, p. 17]. Note that the factor 2 in the reaction rate accounts for B^2 rather than B appearing in t_s.

We have chosen not to rescale the mass fraction Y (which was already dimensionless) because the above choices already simplify the equations as much as we want. Although the additional scaling of Y that we have at our disposal, is welcome from a mathematical point of view, using it obscures the physical role of the control parameters Y_f and/or T_f. Our motivation for the above choices is that we have at hand two important radiative parameters, namely

$$\alpha = \frac{r_s}{L} = \frac{D\rho}{BL},$$

which is a dimensionless opacity, and

$$\beta = \frac{F_s t_s}{\rho C_p T_s r_s} = \frac{4\sigma_{\mathrm{sb}} Q^3 D^4 \rho^4}{\lambda^4 B},$$

which is a measure of the radiative flux compared to the convective flux. Furthermore, there is the Lewis number

$$\mathrm{Le} = \frac{r_2^2}{Dt_s} = \frac{\lambda}{\rho C_p D},$$

a diffusion parameter. In the new variables the system becomes (where we drop the hats from the notation)

$$\begin{aligned} Y_t - \frac{1}{\mathrm{Le}}\Delta Y &= 0, \quad z < s(y,t); \qquad Y \equiv 0, \quad z \geq s(y,t); \\ T_t - \Delta T + \beta \nabla \cdot \mathbf{F_R} &= 0, \quad z \neq s(y,t); \\ -\nabla(\nabla \cdot \mathbf{F_R}) + 3\alpha^2 \mathbf{F_R} + \alpha \nabla T^4 &= 0. \end{aligned}$$

The jump conditions at the free boundary $z = s(y,t)$ are

$$\left[\frac{\partial Y}{\partial n}\right] = \mathrm{Le}\,\omega(T) \quad \text{and} \quad \left[\frac{\partial T}{\partial n}\right] = -\omega(T) \qquad \text{at } z = s(y,t),$$

with non-dimensional chemical reaction rate (still denoted by ω)

$$\omega(T) = \exp\left(N\left(\frac{1}{T_c} - \frac{1}{T}\right)\right),$$

where

$$N = \frac{E}{2RT_s}$$

is the dimensionless activation energy, and $T_c = T_C/T_s$ is the dimensionless characteristic temperature, the significance of which was already discussed in the introduction.

2.3 Planar travelling waves

We consider flames modelled by planar (one-dimensional) travelling wave solutions and we thus introduce the travelling wave coordinate is $x = z + \mu t$, describing waves travelling at speed μ to the left (into the fresh region). In such a travelling wave the radiative flux has only one component, which we rescale by β for convenience:

$$\mathbf{F_R} = (q/\beta, 0, 0).$$

Also, we introduce the new combined parameter

$$\chi = \alpha\beta.$$

Finally, we may reposition the free boundary at the origin. This leads to the system

$$\mu Y' - \frac{1}{\mathrm{Le}} Y'' = 0, \quad x < 0; \qquad Y \equiv 0, \quad x \geq 0; \tag{10a}$$

$$\mu T' - T'' + q' = 0, \quad x \neq 0; \tag{10b}$$

$$-q'' + 3\alpha^2 q + \chi (T^4)' = 0, \quad x \in \mathbb{R}. \tag{10c}$$

The jump conditions at $x = 0$ are

$$[Y] = [T] = [q] = [q'] = 0, \tag{10d}$$

$$[T'] = -\omega(T), \quad [Y'] = \mathrm{Le}\, \omega(T), \tag{10e}$$

and $\omega(T)$ is still given by

$$\omega(T) = \exp\left(N \left(\frac{1}{T_c} - \frac{1}{T} \right) \right). \tag{10f}$$

Note that the equation (10c) for q implies the continuity of q and q'. The conditions at infinity are

$$T(-\infty) = T_-, \quad Y(-\infty) = Y_-, \quad T(+\infty) = T_+, \quad q(\pm\infty) = 0, \tag{10g}$$

in which $Y_- = Y_f$ is the (dimensionless) "fresh" mass fraction, T_- is the dimensionless fresh temperature and T_+ the dimensionless burnt temperature. In fact, direct integration of the equations (see Section 3) shows that

$$T_+ = T_- + Y_-. \tag{11}$$

This conservation law (cf. [3, p.221]) reflects the fact that physically only the conditions in the fresh region can be controlled, whereas the temperature in the burnt region is determined by the reaction. The conservation law relating the asymptotic temperatures and fuel mass fraction is independent of the radiation parameters, so that the temperature far behind the flame front is nothing but the adiabatic flame temperature (in absence of radiation effects the temperature behind the flame is uniform $T \equiv T_{ad} = T_- + Y_-$). The limiting behaviour for q at infinity means that radiative equilibrium is achieved at infinity. This follows naturally from (10c); in fact, q may be expressed in terms of T^4 by a convolution formula with a Green's function.

From [4] we know the existence of a travelling wave solution

$$(Y(x), T(x), q(x), \mu)$$

of the system (10) for all (positive) values of the parameters, provided the conservation law (11) is satisfied. Every solution satisfies

$$T_- \leq T(x) \leq T_- + 2Y_-.$$

It is remarkable that this bound is independent of the other parameters.

3 Matched asymptotic analysis

3.1 Setting the stage

In this section we evaluate the simultaneous asymptotic regime of high activation energy and highly radiative flames. We thus introduce *three* small parameters:

$$\varepsilon = N^{-1}$$
$$\delta_1 = \chi = \alpha\beta$$
$$\delta_2 = 3\beta^{-2}.$$

We will couple δ_1 and δ_2 to ε in a moment.

First, we remark that the equation for Y decouples and can be solved explicitly:

$$Y(x) = Y_-(1 - e^{\mathrm{Le}\mu x}), \quad x < 0; \qquad Y(x) = 0, \quad x \geq 0. \tag{13}$$

The jump condition for Y' leads to an expression for the flame velocity:

$$\mu = \frac{1}{Y_-}\exp\left(N\left(\frac{1}{T_c} - \frac{1}{T^*}\right)\right). \tag{14}$$

Since the remaining problem for T, q and μ is independent of the Lewis number Le, it does not appear in the subsequent asymptotic analysis. However, it plays an important role in the stability analysis, which we discuss in a forthcoming paper [2].

Since Y is given by (13), the system (10a)–(10c) reduces to a set of two equations

$$T'' = \mu T' + q',$$
$$q'' = 3\alpha^2 q + \chi(T^4)'.$$

The first equation can be integrated once, but since T' is discontinuous at $x = 0$, the integration cannot be across the origin. We therefore integrate starting from $x = \infty$ for positive x, while starting from $x = -\infty$ for negative x. This leads to

$$T' = \mu(T - T_\pm) + q \qquad \text{for } x \neq 0.$$

Here and throughout the paper $T_\pm$ stands for T_+ on the right ($x > 0$) and T_- on the left ($x < 0$). We note that we will frequently have to treat the equations separately on the right and on the left.

Using the notation (12) the system reads

$$T' = \mu(T - T_\pm) + q, \tag{15a}$$
$$q'' = \delta_1^2\delta_2 q + \delta_1(T^4)', \tag{15b}$$

with "boundary conditions" at infinity

$$T(-\infty) = T_-, \quad T(+\infty) = T_+, \quad q(\pm\infty) = 0,$$

and at the origin T, q and q' are continuous, while T' satisfies the jump condition

$$\mu(T_- - T_+) = [T'] = -\mu Y_-. \tag{16}$$

The first equality stems from (15a), while the second equality is a consequence of the jump conditions (10e) and the explicit expression (13) for Y. The two equalities in (16) reflect the conservation law

$$T_+ = T_- + Y_-. \tag{17}$$

Here and in what follows we assume that μ is order 1, so that we are dealing with asymptotically finite speeds of propagation. The system (15) now naturally leads to the expansion

$$T \sim T_0 + \delta_1 T_1 + \delta_2 T_2 + \delta_1^2 T_3 + \delta_1\delta_2 T_4,$$
$$q \sim q_0 + \delta_1 q_1 + \delta_2 q_2 + \delta_1^2 q_3 + \delta_1\delta_2 q_4.$$

In view of (14) our overriding interest is in the temperature at the free boundary. Therefore we introduce the notation $T_i^* = T_i(0)$ for $i = 0, 1, 2$, hence

$$T(0) = T^* \sim T_0^* + \delta_1 T_1^* + \delta_2 T_2^*.$$

In this new notation the relation (14) between the flame velocity μ and the flame temperature T^* reads

$$\ln(\mu Y_-) \sim \frac{1}{\varepsilon}\left(\frac{1}{T_c} - \frac{1}{T_0^* + \delta_1 T_1^* + \delta_2 T_2^*}\right). \tag{18}$$

There are now several straightforward remarks to make. For the terms on the right and left to balance (i.e. for a finite propagation speed) one needs

$$T_c = T_0^*.$$

This reduces (18) to

$$\ln(\mu Y_-) \sim -\frac{\delta_1}{\varepsilon}\frac{T_1^*}{(T_0^*)^2} - \frac{\delta_2}{\varepsilon}\frac{T_2^*}{(T_0^*)^2}. \tag{19}$$

We anticipate (see below) that $T_1^* < 0$ and $T_2^* < 0$, so the right-hand side of (19) is always nonzero. It is now immediate that we need

$$\delta_1 = O(\varepsilon) \qquad \text{and} \qquad \delta_2 = O(\varepsilon).$$

If both $\delta_1 \ll \varepsilon$ and $\delta_2 \ll \varepsilon$ then we just have $\mu = 1/Y_-$. If δ_1 and/or δ_2 are of order ε then the left- and right-hand sides balance and the results announced in the introduction follow. Of course, they follow only after we have found the expressions for T_0^*, T_1^* and T_2^*, which are (we will spend the rest of this section establishing this, see (39), (44) and (45)):

$$T_0^* = T_+ + Y_-;$$
$$T_1^* = -\mu^{-2}\big(8T_+^3 Y_- + 9T_+^2 Y_-^2 + \frac{16}{3}T_+ Y_-^3 + \frac{5}{4}Y_-^4\big);$$
$$T_2^* = -\frac{\mu^2}{4T_+^5}\int_0^{Y_-/T_+} \frac{t}{(t+1)^4 - 1}\,dt - \frac{\mu^2 Y_-}{16T_+^6}.$$

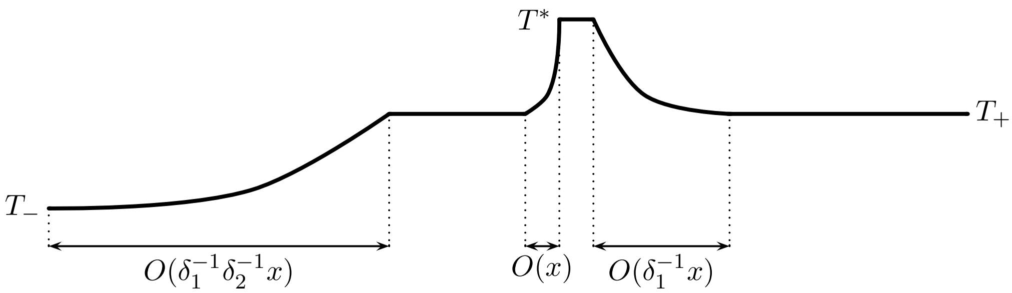

Figure 4: The three different scales of the asymptotic problem. The shape of the profiles shown of course uses some a posteriori knowledge which will be collected in the matched asymptotic analysis in Sections 3.2–3.4.

To calculate T_0^*, T_1^* and T_2^* we have to match the profile that we obtain on the scale $x = O(1)$ to *two* larger scales. The scale at order $x = O(1)$ we call the inner region, $x = O(\delta_1^{-1})$ is the intermediate region, and $x = O(\delta_1^{-1}\delta_2^{-1})$ is the outer region (see also Figure 4). One may wonder why we do not have a scale $x = O(\delta_2^{-1})$. The reason is that the profile turns out to be flat at this scale and therefore no useful information can be extracted. Throughout we calculate with δ_1 and δ_2 as independent quantities. That they are possibly of the same order in ε does not matter whatsoever for the calculations.

In the intermediate and remote regions introduced above the variables are

$$\begin{aligned} \text{intermediate: } \hat{x} &= \delta_1 x, \qquad \hat{T}(\hat{x}) = T(x) \text{ and } \hat{q}(\hat{x}) = q(x); \\ \text{outer: } \tilde{x} &= \delta_1\delta_2 x, \qquad \tilde{T}(\tilde{x}) = T(x) \text{ and } \tilde{q}(\tilde{x}) = q(x). \end{aligned}$$

(This means $\tilde{x}$ is a factor 3 larger than announced in the introduction, alas.) Although we are eventually interested at the value of T at the origin in the inner region, we start our analysis in the outer region, since there we know the boundary conditions:

$$\lim_{\hat{x}\to\pm\infty} \hat{T}(\hat{x}) = T_\pm \qquad \text{and} \qquad \lim_{\hat{x}\to\pm\infty} \hat{q}(\hat{x}) = 0.$$

We are thus going to work from the outside inwards.

3.2 The outer region

The problem in the outer region is

$$\begin{aligned} \delta_1\delta_2\tilde{T}' &= \mu(\tilde{T} - T_\pm) + \tilde{q}, \\ \delta_2\tilde{q}'' &= \tilde{q} + (\tilde{T}^4)', \end{aligned}$$

with boundary conditions

$$\tilde{T}(\pm\infty) = T_\pm \qquad \text{and} \qquad \tilde{q}(\pm\infty) = 0.$$

Of course these equations must be solved on the right and on the left separately, because there are an intermediate as well as an inner region in between. At this outer scale the expansion for $\tilde{T}$ is

$$\tilde{T} = \tilde{T}_0 + \delta_1\tilde{T}_1 + \delta_2\tilde{T}_2,$$

with an analogous expansions for $\tilde{q}$.

The problem for $\tilde{T}_0$ and $\tilde{q}_0$ is

$$\begin{cases} 0 = \mu(\tilde{T}_0 - T_\pm) + \tilde{q}_0, \\ 0 = \tilde{q}_0 + (\tilde{T}_0^4)', \\ \tilde{T}_0(\pm\infty) = T_\pm,\ \tilde{q}_0(\pm\infty) = 0. \end{cases}$$

Combining the equations we get

$$\tilde{T}_0' = \frac{\mu(\tilde{T}_0 - T_\pm)}{4\tilde{T}_0^3}, \qquad \text{with } \tilde{T}_0(\pm\infty) = T_\pm. \tag{20}$$

On the right, the solution is constant:

$$\tilde{T}_0(\tilde{x}) = T_+ \quad \text{and} \quad \tilde{q}_0(\tilde{x}) = 0 \qquad \text{for } \tilde{x} > 0. \tag{21}$$

This follows from the fact that no exponentially growing terms can be present, since it is impossible to match those to the next scale. This argument is silently used several times in what follows.

On the left, we have a choice of the constant solution, an increasing solution and a decreasing solution. As it turns out, the increasing solution will be the one we need. It starts from T_- at $\tilde{x} = -\infty$ and since equation (20) is autonomous, the solution can be translated and hence the value at the origin is a priori unknown. It has to be determined by matching with the intermediate region. For now, we just introduce the undetermined constant

$$\tilde{T}_0^* \stackrel{\text{def}}{=} \lim_{\tilde{x}\uparrow 0} \tilde{T}_0(\tilde{x}).$$

In order to match with the intermediate region we will need the asymptotic behaviour near the origin, which in terms of $\tilde{T}_0^*$ is given by

$$\tilde{T}_0(\tilde{x}) \sim \tilde{T}_0^* + \frac{\mu(\tilde{T}_0^* - T_-)}{4\tilde{T}_0^{*3}}\, \tilde{x} \qquad \text{as } \tilde{x} \uparrow 0, \tag{22}$$

and $\tilde{q}_0(\tilde{x}) = \mu(\tilde{T}_0(\tilde{x}) - T_-)$ for $\tilde{x} < 0$.

Next, the problem for $\tilde{T}_1$ and $\tilde{q}_1$ (at order δ_1) is

$$\begin{cases} 0 = \mu\tilde{T}_1 + \tilde{q}_1, \\ 0 = \tilde{q}_1 + (4\tilde{T}_0^3\tilde{T}_1)', \\ \tilde{T}_1(\pm\infty) = 0,\ \tilde{q}_1(\pm\infty) = 0. \end{cases}$$

The limit behaviour as $\tilde{x} \to \pm\infty$ is trivial since $T_\pm$ are independent of δ_1 (and δ_2). As it turns out, we only need the solution on the right. There $\tilde{T}_0 = T_+$, so the two equations can be reduced to

$$\tilde{T}_1' = \frac{\mu\tilde{T}_1}{4T_+^3}, \qquad \text{with } \tilde{T}_1(+\infty) = 0,$$

hence the solution is simply

$$\tilde{T}_1 = \tilde{q}_1 = 0 \qquad \text{for } \tilde{x} > 0. \tag{23}$$

Similarly, the problem for $\tilde{T}_2$ and $\tilde{q}_2$ is

$$\begin{cases} 0 = \mu\tilde{T}_2 + \tilde{q}_2, \\ \tilde{q}_0 = \tilde{q}_2 + (4\tilde{T}_0^3\tilde{T}_2)', \\ \tilde{T}_2(\pm\infty) = 0,\ \tilde{q}_2(\pm\infty) = 0. \end{cases}$$

Again, we only need the solution on the right, which is simply

$$\tilde{T}_2 = \tilde{q}_2 = 0 \qquad \text{for } \tilde{x} > 0. \tag{24}$$

3.3 The intermediate problem

At the intermediate scale the problem reads

$$\begin{aligned} \delta_1\hat{T}' &= \mu(\hat{T} - T_\pm) + \hat{q}, \\ \hat{q}'' &= \delta_2\hat{q} + (\hat{T}^4)', \end{aligned}$$

with boundary conditions for $\hat{x} \to -\infty$

$$\begin{aligned} \hat{T}(\hat{x}) &= \tilde{T}_0^* + \delta_1 O(\hat{x}^0) + \delta_2[\tfrac{\mu(\tilde{T}_0^* - T_-)}{4\tilde{T}_0^{*3}}\hat{x} + O(\hat{x}^0)] + o(\delta_1, \delta_2); \\ \hat{q}(\hat{x}) &= -\mu(\tilde{T}_0^* - T_-) + \delta_1 O(\hat{x}^0) + \delta_2[-\tfrac{\mu^2(\tilde{T}_0^* - T_-)}{4\tilde{T}_0^{*3}}\hat{x} + O(\hat{x}^0)] + o(\delta_1, \delta_2); \end{aligned} \tag{25}$$

and for $\hat{x} \to \infty$

$$\begin{aligned} \hat{T}(\hat{x}) &= T_+ + o(\delta_1, \delta_2); \\ \hat{q}(\hat{x}) &= o(\delta_1, \delta_2). \end{aligned} \tag{26}$$

These boundary conditions are determined by the outer solution, namely (22) leads to (25), while (21), (23) and (24) imply (26). At the intermediate scale the expansion for $\hat{T}$ is

$$\hat{T} = \hat{T}_0 + \delta_1\hat{T}_1 + \delta_2\hat{T}_2,$$

with an analogous expansions for $\hat{q}$.

The problem for $\hat{T}_0$ and $\hat{q}_0$ is

$$\begin{cases} 0 = \mu(\hat{T}_0 - T_\pm) + \hat{q}_0, \\ \hat{q}_0'' = (\hat{T}_0^4)', \\ \hat{T}_0(-\infty) = \tilde{T}_0^*,\ \hat{q}_0(-\infty) = -\mu(\tilde{T}_0^* - T_-), \\ \hat{T}_0(+\infty) = T_+,\ \hat{q}_0(+\infty) = 0. \end{cases}$$

The two equations can be combined into

$$\mu\hat{T}_0'' + (\hat{T}_0^4)' = 0. \tag{27}$$

On the left, we integrate from $\hat{x} = -\infty$ and obtain $\mu\hat{T}_0' + \hat{T}_0^4 - \tilde{T}_0^{*4} = 0$. Since $\hat{T}_0(-\infty) = \tilde{T}_0^*$ the solution on the left is

$$\hat{T}_0(\hat{x}) = \tilde{T}_0^* \quad \text{and} \quad \hat{q}_0(\hat{x}) = -\mu(\tilde{T}_0^* - T_-) \qquad \text{for } \hat{x} < 0. \tag{28}$$

On the right, integration of (27) from $\hat{x} = \infty$ gives

$$\mu \hat{T}_0' = -\hat{T}_0^4 + T_+^4, \qquad \text{with } \hat{T}_0(+\infty) = T_+. \tag{29}$$

This situation is very similar to that in the left outer region. We have a choice of the constant solution, an increasing solutions and a decreasing solution, and it is this last one we need. Since the equation is autonomous, the solution can be translated and hence the value at the origin is a priori unknown. It has to be determined by matching with the inner region. Again, we introduce an undetermined constant

$$\hat{T}_0^* \stackrel{\text{def}}{=} \lim_{\hat{x} \downarrow 0} \hat{T}_0(\hat{x}).$$

For the asymptotic behaviour near $\hat{x} = 0$ we get, using (27) and (29),

$$\hat{T}_0(\hat{x}) \sim \hat{T}_0^* - \mu^{-1}(\hat{T}_0^{*4} - T_+^4)\,\hat{x} + 2\mu^{-2}\hat{T}_0^{*3}(\hat{T}_0^{*4} - T_+^4)\,\hat{x}^2 \qquad \text{as } \hat{x} \downarrow 0, \tag{30}$$

and of course $\hat{q}_0(\hat{x}) = -\mu(\hat{T}_0(\hat{x}) - T_+)$ for $\hat{x} > 0$.

The problem for $\hat{T}_1$ and $\hat{q}_1$ is

$$\begin{cases} \hat{T}_0' = \mu \hat{T}_1 + \hat{q}_1, \\ \hat{q}_1'' = (4\hat{T}_0^3 \hat{T}_1)', \\ \hat{T}_1(\pm\infty) = 0, \ \hat{q}_1(\pm\infty) = 0. \end{cases}$$

On the left, the equation reduces to $\mu \hat{T}_1'' + 4\tilde{T}_0^{*3}\hat{T}_1' = 0$, hence the solution is constant. The value of the constant is unknown at this point. Since we shortly have to match with the inner region, we use the undetermined limit value at the origin $\hat{T}_1^- \stackrel{\text{def}}{=} \hat{T}_1(0^-)$ to denote the constant:

$$\hat{T}_1(\hat{x}) = \hat{T}_1^- \quad \text{and} \quad \hat{q}_1(\hat{x}) = -\mu \hat{T}_1^- \qquad \text{for } \hat{x} < 0. \tag{31}$$

On the right, one obtains $\mu \hat{T}_1'' = -4(\hat{T}_0^3 \hat{T}_1)' + \hat{T}_0'''$. Integrating from 0 to ∞ we get, using (30) and setting $\hat{T}_1^+ \stackrel{\text{def}}{=} \hat{T}_1(0^+)$,

$$\hat{T}_1'(0^+) = -4\mu^{-1}\hat{T}_0^{*3}\hat{T}_1^+ + 4\mu^{-3}\hat{T}_0^{*3}(\hat{T}_0^{*4} - T_+^4). \tag{32}$$

This equation expresses $\hat{T}_1'(0^+)$ in the unknown constant $\hat{T}_1^+$. The behaviour of $\hat{q}_1$ near the origin is given by

$$\begin{aligned} \hat{q}_1(\hat{x}) &\sim \hat{T}_0'(0^+) - \mu \hat{T}_1^+ + (\hat{T}_0''(0^+) - \mu \hat{T}_1'(0^+))\,\hat{x} \\ &\sim -\mu^{-1}(\hat{T}_0^{*4} - T_+^4) - \mu \hat{T}_1^+ + 4\hat{T}_0^{*3}\hat{T}_1^+\,\hat{x} \qquad \text{as } \hat{x} \downarrow 0. \end{aligned}$$

The problem for $\hat{T}_2$ and $\hat{q}_2$ is

$$\begin{cases} 0 = \mu \hat{T}_2 + \hat{q}_2, \\ \hat{q}_2'' = \hat{q}_0 + (4\hat{T}_0^3 \hat{T}_2)', \\ \hat{T}_2(+\infty) = 0, \ \hat{q}_2(+\infty) = 0, \\ \hat{T}_2'(-\infty) = \frac{\mu(\tilde{T}_0^* - T_-)}{4\tilde{T}_0^{*3}}, \ \hat{q}_2'(-\infty) = -\frac{\mu^2(\tilde{T}_0^* - T_-)}{4\tilde{T}_0^{*3}}. \end{cases}$$

On the left, the equation reduces to $\mu\hat{T}_2'' = -4\tilde{T}_0^{*3}\hat{T}_2' + \mu(\tilde{T}_0^* - T_-)$, with solution, setting as usual $\hat{T}_2^- \stackrel{\text{def}}{=} \hat{T}_2(0^-)$,

$$\hat{T}_2(\hat{x}) = \hat{T}_2^- + \tfrac{\mu(\tilde{T}_0^* - T_-)}{4\tilde{T}_0^{*3}}\hat{x} \quad \text{and} \quad \hat{q}_2(\hat{x}) = -\mu\hat{T}_2^- - \tfrac{\mu^2(\tilde{T}_0^* - T_-)}{4\tilde{T}_0^{*3}}\hat{x} \qquad \text{for } \hat{x} < 0. \tag{33}$$

On the right, the equation becomes $\mu\hat{T}_2'' = -(4\hat{T}_0^3\hat{T}_2)' + \mu(\hat{T}_0 - T_+)$. Integrating from 0 to ∞ we get, setting $\hat{T}_2^+ \stackrel{\text{def}}{=} \hat{T}_2(0^+)$,

$$\hat{T}_2'(0^+) = -4\mu^{-1}\hat{T}_0^{*3}\hat{T}_2^+ - \int_0^\infty \big[\hat{T}_0(\hat{x}) - T_+\big]\, d\hat{x} \tag{34a}$$

The last integral involves the function $\hat{T}_0(\hat{x})$, which we have not computed explicitly. The integral can be simplified using equation (29) for $\hat{T}_0$:

$$\begin{aligned} I_2 &\stackrel{\text{def}}{=} \int_0^\infty \big[\hat{T}_0(\hat{x}) - T_+\big]\, d\hat{x} = -\int_0^{\hat{T}_0^* - T_+} \frac{\hat{T}_0 - T_+}{(\hat{T}_0 - T_+)'}\, d(\hat{T}_0 - T_+) \\ &= \frac{\mu}{T_+^2}\int_0^{\hat{T}_0^*/T_+ - 1} \frac{t}{(t+1)^4 - 1}\, dt. \end{aligned} \tag{34b}$$

We could compute the primitive, but that does not lead to more insight. Finally, the behaviour of $\hat{q}_2$ near the origin is given by

$$\hat{q}_2(\hat{x}) \sim -\mu\hat{T}_2^+ + [4\hat{T}_0^{*3}\hat{T}_2^+ + \mu I_2]\,\hat{x} \qquad \text{as } \hat{x} \downarrow 0.$$

3.4 The inner problem

We are getting to the core of the problem. In the inner scale we want to solve

$$\begin{aligned} T' &= \mu(T - T_\pm) + q, \\ q'' &= \delta_1^2\delta_2 q + \delta_1(T^4)'. \end{aligned}$$

The boundary conditions are for $x \to -\infty$:

$$\begin{aligned} T(x) &= \tilde{T}_0^* + \delta_1\hat{T}_1^- + \delta_2\hat{T}_2^- + \delta_1^2 O(x^0) \\ &\qquad + \delta_1\delta_2[\tfrac{\mu(\tilde{T}_0^* - T_-)}{4\tilde{T}_0^{*3}}x + O(x^0)] + o(\delta_1^2, \delta_1\delta_2, \delta_2); \\ q(x) &= -\mu(\tilde{T}_0^* - T_-) - \delta_1\mu\hat{T}_1^- - \delta_2\mu\hat{T}_2^- + \delta_1^2 O(x^0) \\ &\qquad - \delta_1\delta_2[\tfrac{\mu^2(\tilde{T}_0^* - T_-)}{4\tilde{T}_0^{*3}}x + O(x^0)] + o(\delta_1^2, \delta_1\delta_2, \delta_2). \end{aligned} \tag{35}$$

For $x \to \infty$ the boundary conditions look complicated:

$$\begin{aligned} T(x) &= \hat{T}_0^* + \delta_1[-\mu^{-1}(\hat{T}_0^{*4} - T_+^4)x + \hat{T}_1^+] + \delta_2\hat{T}_2^+ \\ &\quad + \delta_1^2\hat{T}_0^{*3}\big[2\mu^{-2}(\hat{T}_0^{*4} - T_+^4)x^2 + 4\{-\mu^{-1}\hat{T}_1^+ + \mu^{-3}(\hat{T}_0^{*4} - T_+^4)\}x + O(x^0)\big] \\ &\quad + \delta_1\delta_2[(-4\mu^{-1}\hat{T}_0^{*3}\hat{T}_2^+ - I_2)x + O(x^0)] + o(\delta_1^2, \delta_1\delta_2, \delta_2); \\ q(x) &= -\mu(\hat{T}_0^* - T_+) + \delta_1[(\hat{T}_0^{*4} - T_+^4)x - \mu^{-1}(\hat{T}_0^{*4} - T_+^4) - \mu\hat{T}_1^+] - \delta_2\mu\hat{T}_2^+ \\ &\quad + \delta_1^2[-2\mu^{-1}\hat{T}_0^{*3}(\hat{T}_0^{*4} - T_+^4)x^2 + 4\hat{T}_0^{*3}\hat{T}_1^+ x + O(x^0)] \\ &\quad + \delta_1\delta_2[(4\hat{T}_0^{*3}\hat{T}_2^+ + \mu I_2)x + O(x^0)] + o(\delta_1^2, \delta_1\delta_2, \delta_2). \end{aligned} \tag{36}$$

These conditions follow from the analysis of the intermediate region, e.g. (35) follows from (28), (31) and (33), whereas (36) follows from (30), (32) and (34). Of course the boundary conditions for $T(x)$ and $q(x)$ as $x \to \pm\infty$ are related through the equation $q = T' - \mu(T - T_\pm)$. Furthermore, at the origin q, q' and T are continuous.

We expand T as

$$T \sim T_0 + \delta_1 T_1 + \delta_2 T_2 + \delta_1^2 T_3 + \delta_1\delta_2 T_4,$$

and analogously for q. We now solve subsequently the equations at zeroth, first and second order in the small parameters δ_1 and δ_2.

3.4.1 Zeroth order

The equations for T_0 and q_0 are

$$\begin{cases} T_0' = \mu(T_0 - T_\pm) + q_0, \\ q_0'' = 0, \\ T_0(-\infty) = \tilde{T}_0^*, \ q_0(-\infty) = -\mu(\tilde{T}_0^* - T_-), \\ T_0(+\infty) = \hat{T}_0^*, \ q_0(+\infty) = -\mu(\hat{T}_0^* - T_+). \end{cases}$$

The functions T_0, q_0 and q_0' are continuous across the origin. This means that $q_0(x)$ is constant, and on the right $T_0(x)$ is constant as well. This implies

$$T_0^* \stackrel{\text{def}}{=} T_0(0) = T_0(+\infty) \qquad \text{and} \qquad q_0(-\infty) = q_0(+\infty),$$

hence, a comparison with the boundary conditions (and (17)) leads to

$$T_0^* = \hat{T}_0^* = \tilde{T}_0^* + T_+ - T_- = \tilde{T}_0^* + Y_-,$$

that is,

$$\hat{T}_0^* = T_0^*, \tag{37a}$$

$$\tilde{T}_0^* = T_0^* - Y_-. \tag{37b}$$

On the left, the solution $T(x)$ decays exponentially to $\tilde{T}_0^* = T_0^* - Y_-$, so

$$T_0(x) = \begin{cases} Y_-(e^{\mu x} - 1) + T_0^* & \text{for } x < 0, \\ T_0^* & \text{for } x \geq 0, \end{cases} \qquad \text{and} \quad q_0(x) = -\mu(T_0^* - T_+).$$

3.4.2 First order

The equations for T_1 and q_1 are (using (37a))

$$\begin{cases} T_1' = \mu T_1 + q_1, \\ q_1'' = (T_0^4)', \\ T_1(-\infty) = \hat{T}_1^-, \ q_1(-\infty) = -\mu\hat{T}_1^-, \\ T_1(x) \sim -\mu^{-1}(T_0^{*4} - T_+^4)x + \hat{T}_1^+ \ \text{ as } x \to \infty, \\ q_1(x) \sim (T_0^{*4} - T_+^4)x - \mu^{-1}(T_0^{*4} - T_+^4) - \mu\hat{T}_1^+ \ \text{ as } x \to \infty. \end{cases}$$

We start by integrating the second equation from $x = -\infty$:

$$q_1'(x) = T_0(x)^4 - T_0(-\infty)^4 = \begin{cases} [Y_-(e^{\mu x} - 1) + T_0^*]^4 - [T_0^* - Y_-]^4, & x < 0, \\ T_0^{*4} - [T_0^* - Y_-]^4, & x \geq 0. \end{cases} \tag{38}$$

We thus have, by comparing with the boundary conditions for q_1 as $x \to \infty$,

$$T_0^{*4} - T_+^4 = q_1'(+\infty) = T_0^{*4} - [T_0^* - Y_-]^4,$$

hence

$$T_0^* = T_+ + Y_-. \tag{39}$$

Although we now have an expression for T_0^*, we keep using the notation T_0^* in the proceeding for notational convenience.

Another integration of (38) from $x = 0$ in both directions gives

$$\begin{aligned} q_1(x) &\to q_1(0) - I_1 && \text{as } x \to -\infty, \\ q_1(x) &= q_1(0) + (T_0^{*4} - T_+^4)\, x && \text{for } x \geq 0, \end{aligned}$$

where

$$I_1 \stackrel{\text{def}}{=} \int_{-\infty}^0 (Y_- e^{\mu x} + T_+)^4 - T_+^4 \, dx = \mu^{-1}\big(4T_+^3 Y_- + 3T_+^2 Y_-^2 + \tfrac{4}{3} T_+ Y_-^3 + \tfrac{1}{4} Y_-^4\big). \tag{40}$$

To obtain $T_1(x)$ on the right we solve $T_1' - \mu T_1 = q_1(0) + (T_0^{*4} - T_+^4)\, x$, and we obtain

$$T_1(x) = T_1^* - \mu^{-1}(T_0^{*4} - T_+^4)\, x \qquad \text{for } x \geq 0, \tag{41}$$

where

$$T_1^* \stackrel{\text{def}}{=} T_1(0) = -\mu^{-1} q_1(0) - \mu^{-2}(T_0^{*4} - T_+^4). \tag{42}$$

On the left, the limit behaviour of T_1 is (using (42))

$$\lim_{x \to -\infty} T_1(x) = -\mu^{-1} q_1(0) + \mu^{-1} I_1 = T_1^* + \mu^{-2}(T_0^{*4} - T_+^4) + \mu^{-1} I_1. \tag{43}$$

Comparing (41) and (43) with the boundary conditions gives the values for $\hat{T}_1^{\pm}$:

$$\begin{aligned} \hat{T}_1^- &= T_1^* + \mu^{-2}(T_0^{*4} - T_+^4) + \mu^{-1} I_1, \\ \hat{T}_1^+ &= T_1^*. \end{aligned}$$

Next, the equation at order δ_2 is

$$\begin{cases} T_2' = \mu T_2 + q_2, \\ q_2'' = 0, \\ T_2(-\infty) = \hat{T}_2^-, \ q_2(-\infty) = -\mu \hat{T}_2^- \\ T_2(+\infty) = \hat{T}_2^+, \ q_2(+\infty) = -\mu \hat{T}_2^+. \end{cases}$$

Since the equations are satisfied on $\mathbb{R}$ the solution is constant, so $\hat{T}_2^- = \hat{T}_2^+ = T_2(0)$ and

$$T_2(x) = T_2^* \stackrel{\text{def}}{=} T_2(0) \qquad \text{for all } x \in \mathbb{R}.$$

3.4.3 Second order

The equation at order δ_1^2 reads

$$\begin{cases} T_3' = \mu T_3 + q_3, \\ q_3'' = 4(T_0^3 T_1)', \\ T_3'(-\infty) = 0, \ q_3'(-\infty) = 0 \\ T_3'(x) \sim 4\mu^{-2} T_0^{*3}(T_0^{*4} - T_+^4)\, x + 4\mu^{-3} T_0^{*3}(-\mu^2 T_1^* + T_0^{*4} - T_+^4) \ \text{ as } x \to \infty \\ q_3'(x) \sim -4\mu^{-1} T_0^{*3}(T_0^{*4} - T_+^4)\, x + 4 T_0^{*3} T_1^* \ \text{ as } x \to \infty. \end{cases}$$

Integrating the second equation from $x = -\infty$ gives

$$q_3'(x) = 4T_0(x)^3 T_1(x) - 4T_+^3 T_1(-\infty)$$

and by using (41) and (43) we obtain for $x \geq 0$

$$q_3'(x) = -4\mu^{-1} T_0^{*3}(T_0^{*4} - T_+^4)x + 4T_0^{*3} T_1^* - 4T_+^3[T_1^* + \mu^{-2}(T_0^{*4} - T_+^4) + \mu^{-1} I_1].$$

Comparing this with the boundary conditions for $q_3'(x)$ as $x \to \infty$ gives

$$T_1^* = -\mu^{-1} I_1 - \mu^{-2}\big((T_+ + Y_-)^4 - T_+^4\big).,\tag{44}$$

with I_1 given in (40).

The equation at order $\delta_1\delta_2$ reads (using (37b))

$$\begin{cases} T_4' = \mu T_4 + q_4, \\ q_4'' = 4(T_0^3 T_2)', \\ T_4'(-\infty) = \frac{\mu Y_-}{4T_+^3}, \ q_4'(-\infty) = -\frac{\mu^2 Y_-}{4T_+^3} \\ T_4'(+\infty) = -4\mu^{-1} T_0^{*3} T_2^* - I_2, \ q_4'(+\infty) = 4T_0^{*3} T_2^* + \mu I_2. \end{cases}$$

Integrating the second equation from $x = -\infty$ to $x = \infty$ gives

$$q_4'(+\infty) - q_4'(-\infty) = 4[T_0^{*3} - T_+^3] T_2^*.$$

On the other hand, the boundary conditions say that

$$q_4'(+\infty) - q_4'(-\infty) = 4T_0^{*3} T_2^* + \mu I_2 + \frac{\mu^2 Y_-}{4T_+^3}.$$

Comparing these expressions for $q_4'(+\infty) - q_4'(-\infty)$ gives

$$T_2^* = -\frac{\mu}{4T_+^3} I_2 - \frac{\mu^2 Y_-}{16 T_+^6}\,,\tag{45}$$

with I_2 given in (34b).

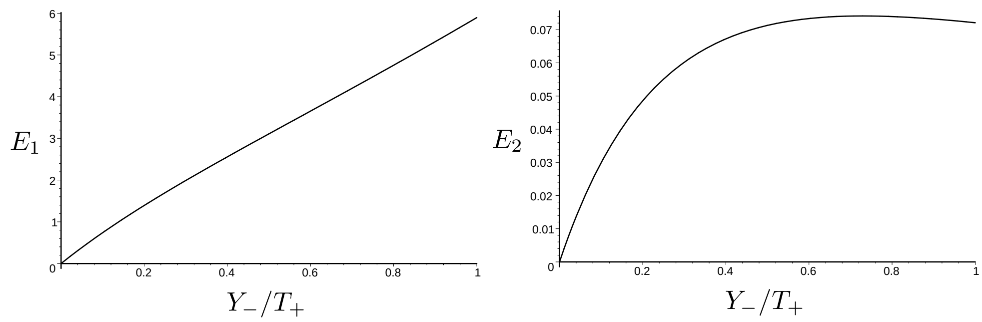

Figure 5: The functions $E_1\left(\frac{Y_-}{T_+}\right)$ and $E_2\left(\frac{Y_-}{T_+}\right)$. Notice that $T_+ = T_- + Y_-$ and thus $0 < \frac{Y_-}{T_+} < 1$.

4 The asymptotic law for the velocity

In this section we take a look at what the speed law tells us. We compare the asymptotic formula with numerical computations for small finite values of ε. In particular, we calculate bifurcation diagrams where the radiative parameters α and β are the continuation parameters. For this, the most delicate case where both terms in the right hand side of (8) are present, is the most interesting, i.e. equation (8a). In this limit the activation energy ε^{-1} is coupled to the radiative parameters via

$$\alpha = \alpha_0 \varepsilon^{3/2} \qquad \text{and} \qquad \beta = \beta_0 \varepsilon^{-1/2}.$$

The relation between the wave speed μ and α_0 and β_0 is thus

$$\ln(\mu Y_-) + \frac{\alpha_0 \beta_0 T_+^2}{\mu^2} E_1\left(\tfrac{Y_-}{T_+}\right) + \frac{\mu^2}{\beta_0^2 T_+^7} E_2\left(\tfrac{Y_-}{T_+}\right) = 0. \tag{46}$$

We note that due to our choice not to scale Y_- (see Section 2.2) this expression should be invariant under the scaling

$$Y_- \to sY_-, \quad T_+ \to sT_+, \quad \mu \to s^{-1}\mu, \quad \alpha_0 \to s^{1/2}\alpha_0, \quad \beta_0 \to s^{-9/2}\beta_0,$$

and it is indeed. Furthermore, if one would replace the nonlinear term T^4 in equation (10c) by a linear approximation, then the solution can be (almost) explicitly calculated for any α and β. In the limit under consideration an expression for the speed law analogous to (46) is founds, see [2]. It is in that context that the stability investigation is being pursued.

The functions E_1 and E_2 depend only on the quotient Y_-/T_+, and since $T_+ = Y_- + T_-$, they thus depend on the ratio of the fuel mass fraction and the dimensionless temperate far ahead of the front. These two functions are plotted in Figure 5.

For the subsequent numerical calculations we need to pick some values for the parameters and we choose $Y_- = T_- = 0.5$ and hence $T_+ = 1$ throughout. The remaining variables in (46) are thus α_0, β_0 and μ. We can plot the surface most easily by writing α_0 as a function of μ and β_0, and the result is shown in Figure 6. When we fix β_0, then for small α_0 there are two solutions which merge in a saddle-node bifurcation as α_0 increases. On the other hand, when we fix α_0 and use β_0 as the bifurcation parameter we see that the set of solutions forms an *isola* in the (β_0, μ)-plane. This means that β_0 has to be carefully selected, not too large and not too small, for a flame with finite propagation speed to exist. If α_0 is too large

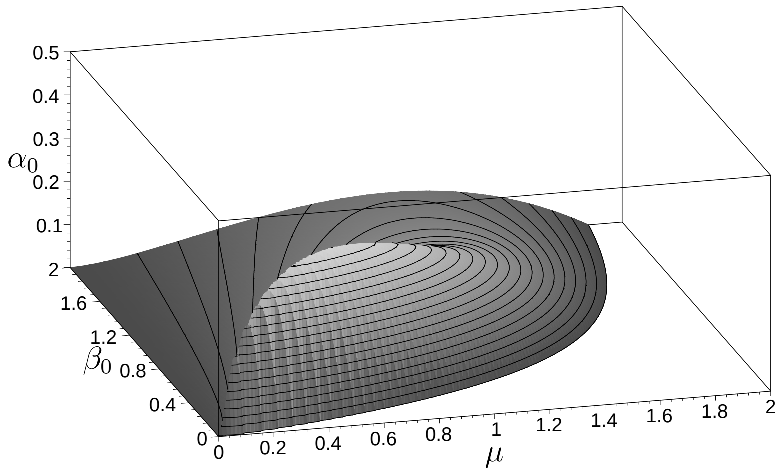

Figure 6: The surface in (μ, α_0, β_0)-space describing the speed law.

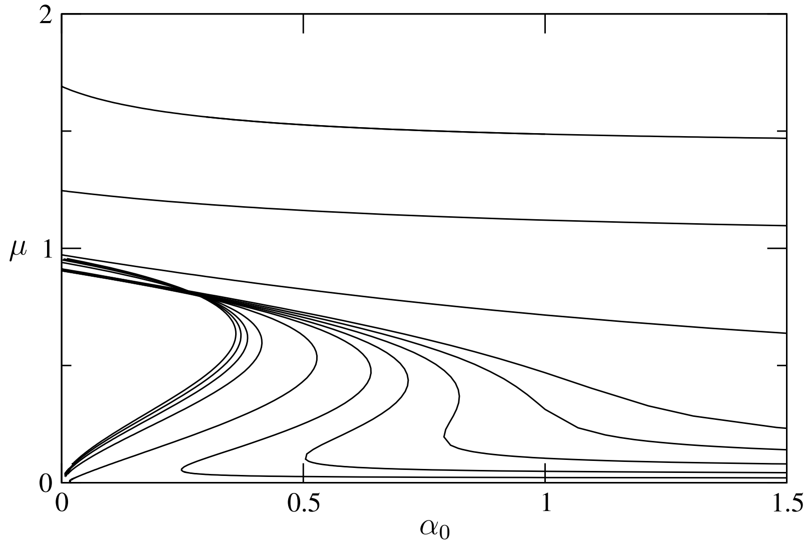

Figure 7: The solution curves in the (α_0, μ)-plane for fixed $\beta_0 = 0.3$ and $\varepsilon = 1, 0.5, 0.2, 0.11, 0.1, 0.09, 0.08, 0.07, 0.05, 0.02, 0.01, 0.005, 0.001$. As ε decreases the solution curves shift inwards, i.e. the curve at the top corresponds to $\varepsilon = 1$.

then there are no travelling waves. The maximum value of α_0 for which solutions exist can be calculated to be

$$\alpha_{\max} = \sqrt{\frac{T_+^3}{2e^3 Y_-^2 E_1^2 E_2}}.$$

To compare the asymptotic analysis with numerical computations, we implemented the travelling wave problem in the AUTO software package [7] for continuation of solution to ODEs. We treated the three different spatial regions with some care to reflect their respective scaling with ε (or with δ_1 and δ_2 to be more precise). We calculated the bifurcation diagram using both α_0 and β_0 as parameters for a set of small values of ε. The resulting pictures are shown in Figures 7 and 8, and one can see how the asymptotic regime is approached. For the (α_0, μ)-diagram the solution curves become S-shaped as ε decreases, and then approach a bell shaped curve as $\varepsilon \to 0$. In the (β_0, μ)-diagram the solution branch curves back more and more and finally it closes on itself as ε approaches 0.

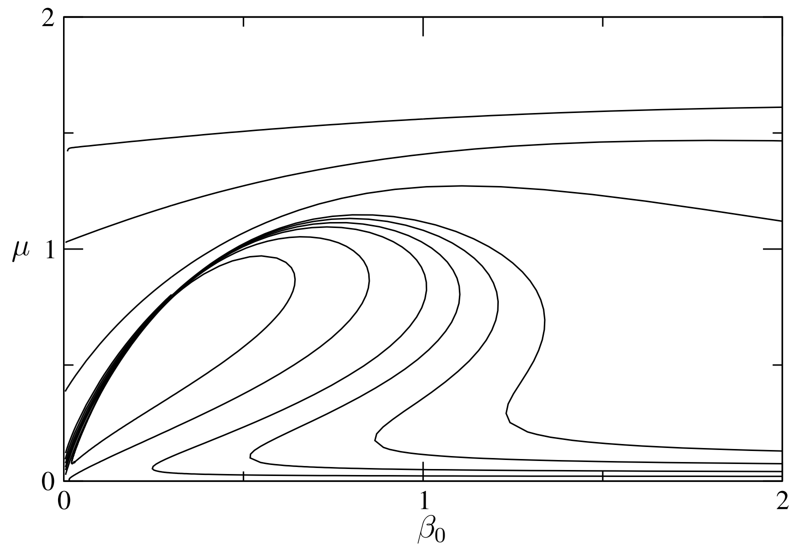

Figure 8: The solution curves in the (β_0, μ)-plane for fixed $\alpha_0 = 0.3$ and the same values of ε as in Figure 7. As ε decreases the solution curves shift inwards.

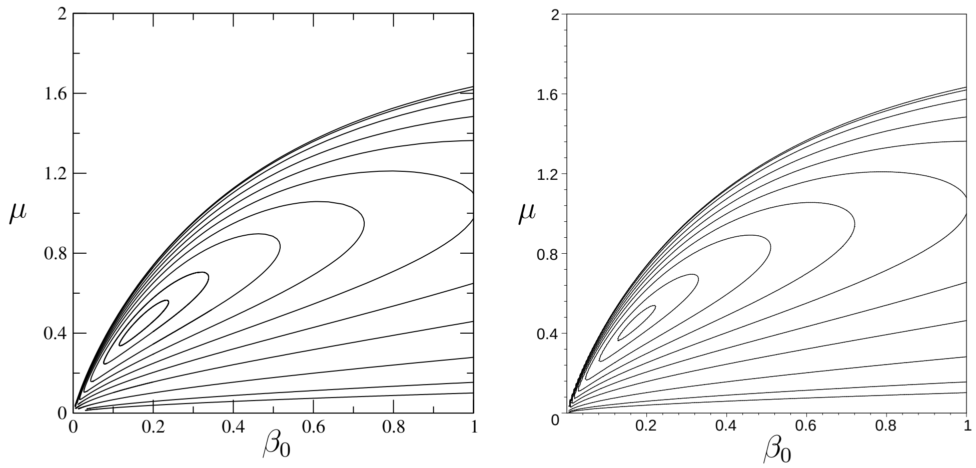

Figure 9: On the left is the (β_0, μ) bifurcation diagram for $\varepsilon = 0.001$ and $\alpha_0 = 0.01, 0.02, 0.05, 0.1, 0.15, 0.2, 0.25, 0.3, 0.35, 0.375$. As α_0 increases the curves are moving inwards. On the right are, for the same set of α_0 values, the contour lines of the surface (see Figure 6) describing the asymptotic speed law as $\varepsilon \to 0$.

To be able to compare with the analytic expression in the limit $\varepsilon \to 0$, we fixed $\varepsilon = 0.001$ and computed the (β_0, μ)-diagram for various values of α_0. The resulting curves can thus be compared with the contour lines of the surface in Figure 6. The numerical computations and the contour lines of the analytic expression are depicted in Figure 9 side by side. The agreement is excellent.

Appendix: the Eddington equation

We consider radiative transfer in a medium of opacity κ at temperature T. A photon travelling at the light speed c covers a distance $L = 1/\kappa$ (the mean free path length of the photon) before being absorbed. Loosely speaking, $L = \infty$ ($\kappa = 0$) corresponds to a transparent medium (optically thin limit) and $L = 0$ ($\kappa = \infty$) to an opaque medium (optically thick limit).

We start from the equation of radiative transfer for the radiative intensity $I = I(\mathbf{r}, \nu, \mathbf{\Omega}, t)$,

$$\frac{1}{c}\frac{\partial I}{\partial t} + \mathbf{\Omega} \cdot \nabla I = \kappa(\mathcal{B}(T, \nu) - I). \tag{47}$$

Here $\mathbf{r}$ is the position, t the time, ν the frequency and $\mathbf{\Omega}$ the unit vector in the direction of propagation. The Planck distribution $\mathcal{B}$ governs the emission of light by the medium and is given by

$$\mathcal{B}(T, \nu) = \frac{2h}{c^2}\frac{\nu^3}{e^{h\nu/(kT)} - 1},$$

where k and h are the Boltzmann and Planck constants.

Since we would like to consider the total amount of radiation, we denote by $\langle \phi \rangle$ the integral of a function ϕ over all frequencies and directions, rescaled with c:

$$\langle \phi \rangle = \frac{1}{c}\int_0^\infty \int_{S^2} \phi(\nu, \mathbf{\Omega})\, d\mathbf{\Omega}\, d\nu.$$

Observing that

$$\langle \mathcal{B}(T) \rangle = aT^4 \quad \text{with} \quad a = \frac{8\pi^5 k^4}{15 h^3 c^3},$$

one obtains from (47) the system [14, 9, 10]

$$\frac{\partial E_R}{\partial t} + \nabla \cdot \mathbf{F_R} = c\kappa(aT^4 - E_R); \tag{48a}$$

$$\frac{1}{c}\frac{\partial \mathbf{F_R}}{\partial t} + c\nabla \mathbf{P_R} = -\kappa \mathbf{F_R}, \tag{48b}$$

for the radiative energy density E_R, the radiative flux $\mathbf{F_R}$ and the radiative pressure $\mathbf{P_R}$, defined by

$$\begin{aligned} E_R &= \langle I \rangle, \\ \mathbf{F_R} &= c\, \langle \mathbf{\Omega}\, I \rangle, \\ \mathbf{P_R} &= \langle \mathbf{\Omega} \otimes \mathbf{\Omega}\, I \rangle. \end{aligned}$$

The factor c is, as is usual, included in the definition of $\mathbf{F_R}$ so that it represent an energy flux. Notice that equations (48) do not form a closed system. They are the first members of a hierarchy, and the system still needs to be closed. If the emission and absorption would be isotropic, then we have

$$\mathbf{F_R} = 0,$$

and also

$$\mathbf{P_R} = \frac{1}{3} E_R \mathbf{Id}. \tag{49}$$

In the so-called "P_1-model", which leads to the Eddington equation, (49) is taken as a closure assumption, so that (48) is replaced by

$$\frac{\partial E_R}{\partial t} + \nabla \cdot \mathbf{F_R} = c\kappa(aT^4 - E_R); \tag{50a}$$

$$\frac{1}{c}\frac{\partial \mathbf{F_R}}{\partial t} + \frac{1}{3} c \nabla E_R = -\kappa \mathbf{F_R}. \tag{50b}$$

Since photons travel at light speed we may assume that the radiation is approximately at steady state at the typical time scale of a moving flame, i.e., the system (50) reduces to

$$\nabla \cdot \mathbf{F_R} = c\kappa(aT^4 - E_R); \qquad \frac{1}{3} c \nabla E_R = -\kappa \mathbf{F_R}.$$

It is not difficult to eliminate one of the unknowns, say E_R, by differentiating the first equation, whence

$$c\kappa \nabla E_R = c\kappa a \nabla(T^4) - \nabla(\nabla \cdot \mathbf{F_R}),$$

so that

$$\nabla(\nabla \cdot \mathbf{F_R}) = 4\kappa\sigma_{\text{sb}} \nabla T^4 + 3\kappa^2 \mathbf{F_R}. \tag{51}$$

Here $\sigma_{\text{sb}} = \frac{1}{4}ac$ is the Stefan-Boltzmann constant.

Equation (51) is the Eddington equation for the radiative flux $\mathbf{F_R}$, which is often written as

$$-L^2 \nabla(\nabla \cdot \mathbf{F_R}) + 3\mathbf{F_R} + 4\sigma_{\text{sb}} L \nabla T^4 = 0.$$

References

[1] Baconneau, O., van den Berg, J.B., Brauner, C.M. & Hulshof, J. 2003 Multiplicity and stability of travelling wave solutions in a free boundary combustion-radiation problem. To appear in EJAM.

[2] van den Berg, J.B., Elrofai, H. & Hulshof, J. Stability analysis of travelling waves in a radiation-combustion free-boundary model for flame propagation. In preparation.

[3] Blouquin, R., Joulin, G. & Merhari, Y. 1997 Combustion regimes of particle-laden gaseous flames: influences of radiation, molecular transports, kinetic-quenching, stoichiometry. *Combust. Theory* **1**, 217–242.

[4] Brauner, C.-M., Hulshof, J. & Ripoll, J.-F. 2001 Existence of travelling wave solutions in a combustion-radiation model. *Discrete and Continuous Dynamical Systems* **1**, 193–208.

[5] Buckmaster, J. & Jackson, T.L. 1994 The effects of radiation on the thermal-diffusive stability boundaries of premixed flames. *Combust. Sci. and Tech.* **103**, 299–313.

[6] Buckmaster, J.D. & Ludford, G.S.S. 1982 *Theory of laminar flames*. Cambridge University Press.

[7] Doedel, E.J., Champneys, A.R., Fairgrieve, T.F., Kuznetsov, Y.A., Sandstede, B. & Wang, X. 1997 *AUTO97, continuation and bifurcation software for ordinary differential equations (with HomCont)*. Available by anonymous ftp from `ftp.cs.concordia.ca`, directory `pub/doedel/auto`.

[8] Dold, J.W., Thatcher, R.W. & Shah, A.A. 2003 High order effects in one step reaction sheet jump conditions for premixed flames. *Combustion theory and modelling* **7**, 109–127.

[9] Dubroca, B. & Feugeas, J.-L. 1999 Etude théorique et numérique d'une hiérarchie de modèles aux moments pour le transfert radiatif. *C. R. Acad. Sci. Paris* **329**, 915–920.

[10] Dubroca, B. & Feugeas, J.-L. 2000 Entropic moment closure hierarchy for the radiative transfer equation. Preprint.

[11] Eddington, A.S. 1926 *The internal constitution of stars*. Cambridge University Press.

[12] Joulin, G. & Deshaies, B. 1986 On radiation-affected flame propagation in gaseous mixtures seeded with inert particles. *Combust. Sci. and Tech.* **47**, 299–315.

[13] Joulin, G. & Eudier, M. 1988 Radiation-dominated propagation and extinction of slow, particle-laden gaseous flames. *22nd Int. Symp. on Combustion* **1**, 1579–1585.

[14] Levermore, C.D. 1996 Moments Closure Hierarchies for Kinetic Theories. *J. Stat. Phys.* **83**, 1021–1065.

[15] Matkowski, B. J. & Sivashinsky, G.I. 1979 On asymptotic derivation of two models in flame theory associated with the constant density approximation. *Siam J. Appl. Math.* **37**, 696–699.

[16] Modest, M.F. 1993 *Radiative heat transfer*. Series in Mechanical Engineering McGraw-Hill, Inc.

[17] Rybicki, G.B. & Lightman, A.P. 1979 *Radiative processes in astrophysics*. John Wiley and Sons.

[18] Williams, F.A. 1994 *Combustion theory*. Addison Wesley.